

Reliability of shear-deficient RC beams strengthened with CFRP-strips

Saleh H. Alsayed, Nadeem A. Siddiqui *

Department of Civil Engineering, King Saud University, Riyadh 11421, Saudi Arabia

HIGHLIGHTS

- Studied the reliability of shear-deficient and shear-strengthened RC beam specimens.
- All the beams were tested until failure to obtain their ultimate load capacities.
- Reliability analysis was carried out for a range of applied loads (service to ultimate).
- Studied the influence of fiber angle; strip width; and strip-spacing on the reliability of beams.

ARTICLE INFO

Article history:

Received 14 September 2012
 Received in revised form 10 January 2013
 Accepted 25 January 2013
 Available online 1 March 2013

Keywords:

Concrete
 CFRP
 Strengthening
 Repair
 Shear-deficient RC beams
 Reliability

ABSTRACT

Effectiveness of externally bonded FRP-strips on the side faces of RC beams in the strengthening of shear-deficient RC beams is well established. However, how the design parameters such as fiber orientation, strip-width, and spacing between the FRP-strips influences the reliability of strengthened beams is not very well known. In the present study, a simplified probabilistic procedure based on Monte Carlo Simulation technique has been presented to study the influence of externally bonded FRP-strips on the reliability of shear-deficient RC beams. To illustrate the procedure, reliability analysis was carried out for the six RC beam specimens of 2 m span. Two of these specimens were shear-deficient control specimens, and the remaining four were the similar beams which were shear-strengthened using CFRP-strips. Out of these four strengthened specimens, in the first two specimens, CFRP-strips were externally bonded at 30° whereas in the other two CFRP-strips were attached at 90° with the longitudinal axis of the beam. All these beams were tested in the lab until failure to obtain their ultimate load carrying capacities. Reliability analysis was then carried out for a range of applied nominal loads, varying from service to ultimate. Three parametric studies (i) effect of fiber orientation; (ii) effect of strip width; and (iii) effect of strip-spacing on reliability of strengthened beams were carried out for two different service loads, taken 60% and 70% of tested beams' capacity. The results indicate that when the service load is 60% (or less) of the ultimate load, beam is sufficiently reliable for all the values of the fiber orientation ranging from 30° to 60° from the longitudinal axis of the beam. However, when the applied load is 70% (or more) of the ultimate load, it is difficult to achieve the desired reliability just by attaching the inclined CFRP strips at a certain angle. The desired reliability, in this case, can be achieved by altering the strip-width or strip-spacing or the both.

© 2013 Elsevier Ltd. All rights reserved.

1. Introduction

FRP may be used on beam or slab soffit to provide additional flexural strength, on the sides of beams to provide additional shear strength [1], or wrapped around columns and beam-column joints to provide confinement and additional ductility, a primary concern in seismic upgrades [2–5]. Over the past decades, a number of theoretical investigations to predict the shear capacity of reinforced concrete beams strengthened externally with FRP with layup laminates or procured strips were done and analytical models were

developed based on different theoretical assumptions and experimental observations. Triantafillou [6] proposed a theoretical model to compute the shear strength capacity of a beam strengthened with externally applied FRP. The 2003 edition of the ACI 440 [7] proposed a theoretical model to compute the enhancement of shear strength of RC beams using external FRP laminates. They focused on the developed effective strain in composites at failure which varies depending upon the variability of composites material properties, dimensions and the application techniques. Mofidi and Chaallal [8] presented the results of an experimental and analytical investigation of shear strengthening of reinforced concrete (RC) beams with externally bonded (EB) fiber-reinforced polymer (FRP) strips and sheets, with emphasis on the effect of the

* Corresponding author. Tel.: +966 1 4676962; fax: +966 1 4677008.
 E-mail address: nadeem@ksu.edu.sa (N.A. Siddiqui).

strip-width-to-strip-spacing ratio on the contribution of FRP (V_f). Razaqpur et al. [9] studied the effects of shear span-to-depth ratio (a/d) and beam depth, or size, on the concrete contribution to the shear resistance of beams longitudinally reinforced with carbon fiber-reinforced polymer (CFRP) bars. One of the distinguishing features of the study was the unsymmetrical nature of the applied load, which created two distinct a/d ratios in the same beam and allowed the effect of the a/d ratio on shear strength to be clearly seen. Suggestions were made for the inclusion of these parameters in the shear design equations. Boushelham and Chaallal [10] assessed the suitability of the limits specified by the guidelines, and proposed an alternative equation as an upper limit for shear strength against web crushing failure. To this end, they developed an analytical approach based on the static theorem of the theory of plasticity. The predictions of the equations resulting from this approach were compared with those obtained from tests reported in the literature and with those predicted by ACI Committee 440-02, Canadian Standard S6-06, and the European recommendations fib TG 9.3. The study showed that the current ACI Committee 440-02 and Canadian Standards provisions are overly conservative and therefore need to be reviewed. Boushelham and Chaalla [11] presented the shear resistance mechanisms involved in RC beams strengthened in shear with externally bonded FRP. Bae et al. [12] investigated the shear performance of RC beams strengthened in shear with externally bonded carbon fiber reinforced polymer (CFRP) strips, subjected to a cyclic loading for 2 million cycles at 2 Hz. Experimental results obtained in this study and the comprehensive review on the existing literature showed that RC beams strengthened in shear with externally bonded CFRP could survive 2 million cycles of cyclic loading without failure.

In the last one decade, a limited research (e.g. [13–15]) was also reported on the reliability of RC beams strengthened with FRP laminates – the first being that of Plevris et al. [16]. These researches are mostly concerned with the flexural reliability of Reinforced Concrete girders and beams strengthened with CFRP laminates.

A detailed review of literature indicates that although a substantial research is available on the experimental and analytical investigations of RC beams strengthened in shear with externally bonded FRP-strips, but simple probabilistic procedures through which one can estimate the risk or reliability of RC beams strengthened in shear with FRP-strips are not widely available. Also the range in which orientation of FRP-strips can provide desired reliability needs to be investigated. The effects of design parameters such as FRP strip-width and strip-spacing on reliability of strengthened beams also require an investigation. Keeping above scope in view, in the present study, a simple probabilistic procedure has been presented to estimate the risk and reliability of RC beams strengthened in shear with CFRP-strips. Reliability was also obtained for a range of fiber orientations to obtain the desired reliability of shear-strengthened RC beams. The influence of the strip-width and the strip-spacing, the parameters which can easily be controlled at the time of strengthening, on the reliability of FRP-strengthened beams is also investigated.

2. Experimental program

2.1. Design of the specimens

In order to carry out the reliability analysis, we require nominal load carrying capacities of shear-deficient and CFRP-strengthened RC beam specimens. For this purpose, six RC beam specimens were designed to be weak in shear and strong in flexure (to direct the failure due to shear only). The cross section and reinforcement details of the specimens are shown in Fig. 1 and Table 1. Out of these six shear-deficient beams specimens, the first two specimens were used as Control specimens and the remaining four specimens were strengthened after attaching the CFRP-strips through epoxy on the side faces of the beam specimens. CFRP-strips were bonded at an angle of 90° (Fig. 2) in the two specimens; whereas they were attached at an angle of 30° (Fig. 3) in the remaining two beams. The strips which were

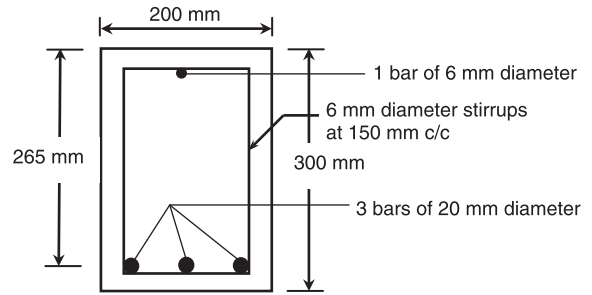


Fig. 1. Cross section and reinforcement details of the beam specimens.

bonded at 90° and those at 30° will be termed as vertical and inclined strips respectively. The nomenclature used for various beam specimens are shown in Table 2. The design of control and CFRP-strengthened specimens were based on ACI 318 [17] and ACI 440.2R-02 [18] respectively. The flexural and shear strength of the beam specimens were estimated and ratio of flexural over shear strength of each beam was determined as presented in Table 3. The ratio in the last column shows that the control specimens are substantially weak in shear, and therefore their failures are very well expected to be in the shear mode. Also for the specimens, strengthened using vertical or inclined strips, still failure is directed to be due to shear as the objective of present strengthening scheme is to study the direct increase in the shear strength and then the reliability due to vertical and inclined-CFRP-strips. By CFRP-strengthening, changing the mode of failure from shear to flexure was not the aim of the present study.

2.2. Material properties

Single batch was used to cast all the specimens. Six cylinders (150 × 300 mm) were cast to determine the average 28-day compressive strength, f'_c , from the batch. The steel bars used as longitudinal and transverse reinforcements were tested to determine their yield strength. The observed average properties of concrete mix and steel bars are shown in Table 4.

The epoxy system used in the study consists of resin and hardener, mixed in a ratio of 3:1. The resin and the hardener were hand mixed thoroughly using a mixing tool for at least 5 min. A thin layer of the epoxy was applied to the concrete surface of 26-day old beam specimen, and CFRP strip was then attached to the surface of the epoxy. Special attention was made to assure that there was no void between the strip and the concrete surface. All CFRP strips used in strengthening were of uni-directional type. After strengthening, the specimens were left at laboratory temperature ($25 \pm 2^\circ\text{C}$ and 30% relative humidity) for 2 days before testing to make sure that the epoxy had enough time to cure. The mechanical properties of the CFRP composite were obtained through the testing of flat coupons. The average mechanical properties, obtained from the average values of the tested coupons, are summarized in Table 4. These values match well with the manufacturer's reported values. Note that the tensile strength was defined based on the cross-sectional area of the coupons, whereas the elastic modulus was calculated from the stress-strain response.

2.3. Preparation of the test specimens

2.3.1. Specimen size and steel reinforcement details

All the beams had a cross section of 200 × 300 mm and a simply supported span of 2000 mm. Out of a total number of six beams, the two beams were used as control specimens and the other four were employed to prepare CFRP-strengthened RC beams. The beams were reinforced with deformed 3Ø20 mm steel bars in tension side and with Ø6 mm steel stirrups @ 150 mm center to center spacing. A Ø6 mm bar was also used in the compression side to tie up the stirrups (Fig. 4). After casting, the specimens were submitted to intermittent spraying of water every day for 2 weeks and then left to dry for the next 2 weeks. On the 26th day after casting, four beams were strengthened by externally bonding the CFRP-strips using epoxy to the concrete surface. The procedure presented below was used for externally bonding the sheets.

2.3.2. Surface treatment phase

The surface of the beam, where the strip was to be attached, was first ground manually and then subjected to a sand blasting to be able to develop a sound bond and withstand the imposed stresses. The process included smoothing out the unevenness in the surface. After smoothing, the surface of the concrete was cleaned with acetone several times until no blackness was found on the washcloth. At this point the strips were also wiped with acetone to remove dust or any adhered substances.

Table 1
Details of the beam specimens.

Designation	Description	Beam size	Bottom steel	Top steel	Stirrups
BC (2 specimens)	Control	200 × 300	3Ø20	1Ø6	Ø6@150 mm
BSV (2 specimens)	Scheme #1	200 × 300	3Ø20	1Ø6	Ø6@150 mm
BSI (2 specimens)	Scheme #2	200 × 300	3Ø20	1Ø6	Ø6@150 mm

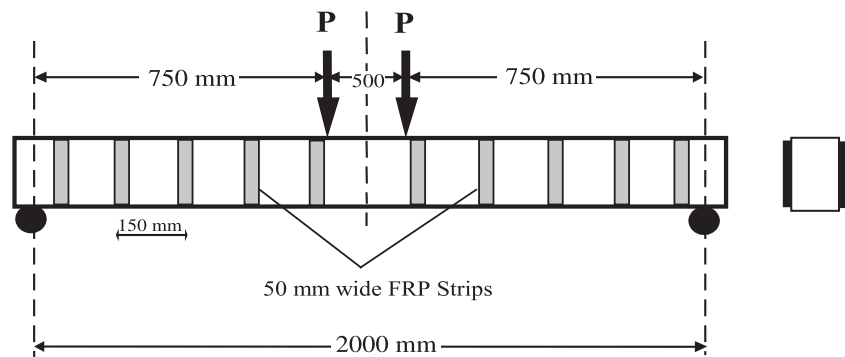


Fig. 2. Schematic diagram of the beam specimen strengthened using vertical CFRP-strips.

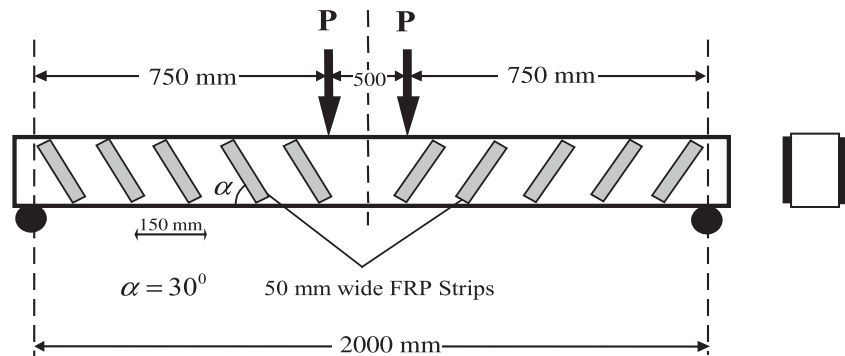


Fig. 3. Schematic diagram of the beam specimen strengthened using inclined CFRP-strips.

Table 2
Nomenclature used and details of the test specimens.

Specimen designation	Number of specimens	Details of strengthening schemes
BC	2	Control beams, weak in shear but strong in flexure.
BSV	2	Strengthened specimens, obtained after the strengthening of another two RC beam specimens using vertical CFRP-strips. The vertical strips were attached through epoxy on the side faces of the beam.
BSI	2	Strengthened specimens, obtained after the strengthening of last two specimens of RC beam specimens using inclined CFRP-strips. The inclined strips were attached through epoxy on the side faces of the beam.

Table 3
Design ratio of shear over flexural strength.

Designation	Description	$P_{uflexure}$ (kN)	P_{ushear} (kN)	$P_{ushear}/P_{uflexure}$
BC	Control	123.2	67.8	0.6
BSV	Strengthened using vertical strips	123.2 ^a	100.9	0.8
BSI	Strengthened using inclined strips	123.2 ^a	113.0	0.9

^a The values shown are for without FRP. To be on conservative side, it is assumed that the shear strengthening of the beams using vertical or inclined CFRP strips does not increase the flexural capacity of the beam.

2.3.3. Attaching the CFRP-strips

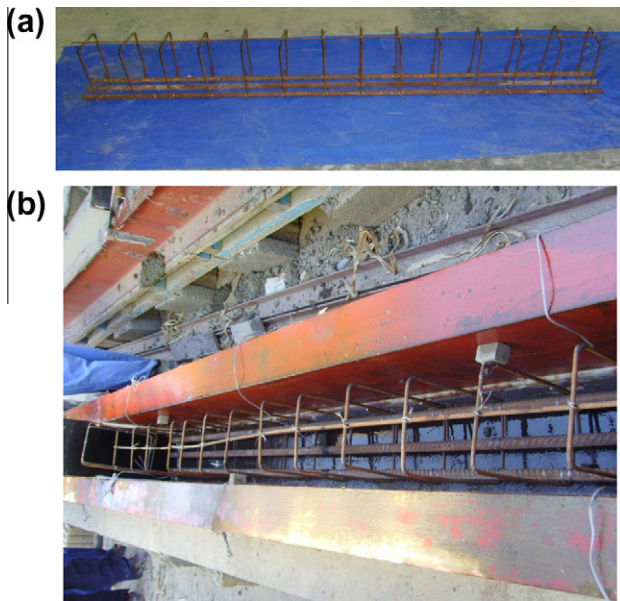
After preparing the concrete surfaces and wiping out the strips, the strips were attached to the concrete surfaces using epoxy. Any excess epoxy was squeezed out by pressing the strips to the concrete. The strips were then kept pressed to the

concrete until hardening. The specimens were kept in the laboratory under control conditions until the day of testing. The strips were attached to the beams as per the designed schemes. In the first scheme, CFRP strips were attached at 90° with respect to the longitudinal axis of the beam, whereas in the second scheme, strips were

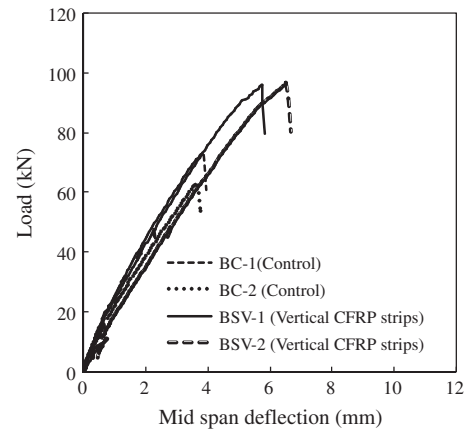
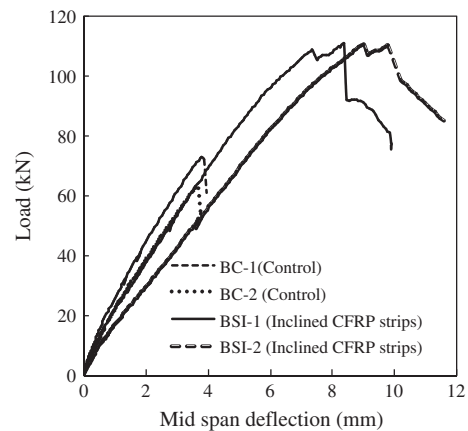
Table 4

Material and geometric properties of the specimens.

Parameter	Nominal value
<i>Concrete and steel</i>	
Concrete strength, f'_c (MPa)	35
Yield strength of longitudinal steel, f_y (MPa)	480
Yield strength of transverse steel, f_{ys} (MPa)	275
Modulus of elasticity of steel, E_s (GPa)	200
<i>CFRP composite system</i>	
Type of FRP	Unidirectional CFRP sheet
Elastic modulus in primary fibers direction	77.3×10^3 MPa
Elastic modulus of CFRP 90° to primary fibers	40.6 MPa
Fracture strain	1.1%
Thickness per layer, t_f	1.0 mm
Width of each strip, w_f	50 mm
Effective depth of FRP strip, d_f	300 mm
No. of FRP layers or plies, n_p	1
Spacing between FRP strips, s_f	150 mm
Inclination of FRP strip with horizontal	30°
<i>Beam dimensions</i>	
Span of the beam, l	2000 mm
Width of the beam, b	200 mm
Depth to steel, d	265 mm
Overall depth of the beam, h	300 mm
Diameter of bottom steel bars	20 mm
Diameter of stirrups	6 mm
Spacing between the stirrups	150 mm

**Fig. 4.** Reinforcement cage used in the preparation of the shear-deficient RC beams.

attached at an angle of 30° from the same axis of the beam. Fig. 5 shows the specimens after the attachment of vertical and inclined strips on the side faces of the beams.

**Fig. 5.** Beams strengthened with the vertical and the inclined CFRP-strips.**Fig. 6.** Load–deflection curves of the control (BC) and the strengthened beams (BSV).**Fig. 7.** Load–deflection curves of the control (BC) and the strengthened beams (BSI).

2.4. Test procedure and setup

The beams were tested using Amsler testing machine with a load control configuration. All the beams were tested simply supported and subjected to two point loads, symmetrically placed at an equal distance from the beam centerline as shown in Figs. 2 and 3. The central deflections were monitored using a linear variable displacement transducer (LVDT). The applied loads and corresponding LVDT deflections were recorded using a data acquisition system. Application of the loads and the recording process continued until the failure of the beam occurred.

2.5. Load–deflection response and failure pattern

The load–deflection response of all the six beams is plotted in Figs. 6 and 7. These figures illustrate the influence of fiber orientation of CFRP strips in upgrading the shear strength of RC beams. The results shown in Fig. 6 indicate that although

the use of vertical strips increases the shear capacity substantially, vertical strips do not add considerable ductility or deformability to beams. Same like the shear-deficient control specimens, a brittle shear failure was observed in the specimens strengthened using vertically attached strips.

The results depicted in Fig. 7 shows the effectiveness of 30° inclined CFRP strips in improving the shear strength of RC beams. This figure clearly indicates that, compared to the response of control beams; the beams retrofitted with CFRP-inclined strips achieve a substantial gain in the strength and show a better deformability. This illustrates the effectiveness of using the inclined strips in the shear-strengthening of RC beams. A better performance of inclined strips over the vertical strips can be attributed to the fact that inclined strips arrest the propagating cracks (due to diagonal tension) in a better way than vertical strips.

A summary of the experimentally observed ultimate loads is given in Table 5. This table shows that, compared to the control beam specimens, beams strengthened with the vertical and inclined strips, show a substantial increase in the shear strength (measured in terms of ultimate load) values. A further comparison of the two shear-strengthening schemes also illustrate that, for the beams strengthened with the inclined (at 30°) CFRP strips, increase in the observed load capacity was almost double (~36%) than the beam strengthened with the vertical strips (~18%). This shows a far better performance of the inclined strips compared to the vertical CFRP strips in the shear strengthening of RC beams.

Figs. 8–10 show the general failure patterns observed in the beam specimens. It was observed that the failure of the control specimen was purely due to the shear as the cracks initiated near the support and propagated almost at 45° with the increase of applied load until failure (Fig. 8). The failure of the beams strengthened with vertical CFRP strips was also brittle due to inclined shear cracks as shown in Fig. 9. The load–displacement curves shown in Fig. 6 indicate the same. This failure pattern shows that although shear strength of beams have been substantially improved (compared to their respective control specimens), but still the beams are weaker in shear than flexure. The failure of the beams strengthened with inclined strips was not as brittle as the beams strengthened with vertical strips (Fig. 10). This indicates that the strengthening of the beams using inclined strips not only impart the strength to the beams but also add some ductility to them. The load–displacement curves shown in Fig. 7 also illustrate the same. The observed cracks (and debonding) were also much less in case of the inclined strips than the vertical strips. In fact, when the applied load was close to the ultimate load, tension bars of the beam were yielded and these yielded bars then experienced some strain hardening, but before arriving at the desired ductile strain limit of 0.005 (ACI 2005), the shear forces reached to the beam's shear capacity and the shear failure took place as shown in Fig. 7. The failure patterns, shown in Figs. 8–10, also indicate that the specimens failed as per the design. In the design of all the specimens, shear strength was kept smaller than the flexural strength as shown in Table 3.

3. Reliability analysis

The reliability assessment of any member of a structure is concerned with the calculation and prediction of its probability of no violation of limit state at any stage during its entire life. In the present study, limit state is said to be violated when shear or flexure capacity of the beam become less than the expected extreme shear force or ultimate bending moment, respectively. In other words, a beam is said to have failed if code specified shear or flexural capacities at the ultimate state of collapse are less than the maximum shear force or ultimate bending moment. In the present study, a Monte Carlo simulation-based procedure has been presented to estimate the probability of failure of beam specimens studied above. A few parametric studies have also been included to obtain the results of practical interest.

3.1. Limit state function

A limit state function is a mathematical representation of a particular limit state of failure. This function assumes a negative or zero value at the failure and a positive value when the member is safe. Thus we can define the probability of limit state violation (i.e. probability of failure) as

$$P_f = P[g(\underline{x}) \leq 0] \quad (1)$$

where $g(\underline{x})$ is the limit state function and \underline{x} is the vector of basic random variables. Keeping above points in view, if the ultimate shear

Table 5
Summary of experimentally observed ultimate loads.

Beam specimens	Observed peak load (kN)	Average peak load P_u (kN)	Increase in ultimate strength with respect to control
BC-1	81.98	81.2	–
BC-2	80.40		
BSV-1	95.97	96.4	18.7%
BSV-2	96.74		
BSI-1	111.01	110.8	36.4%
BSI-2	110.53		

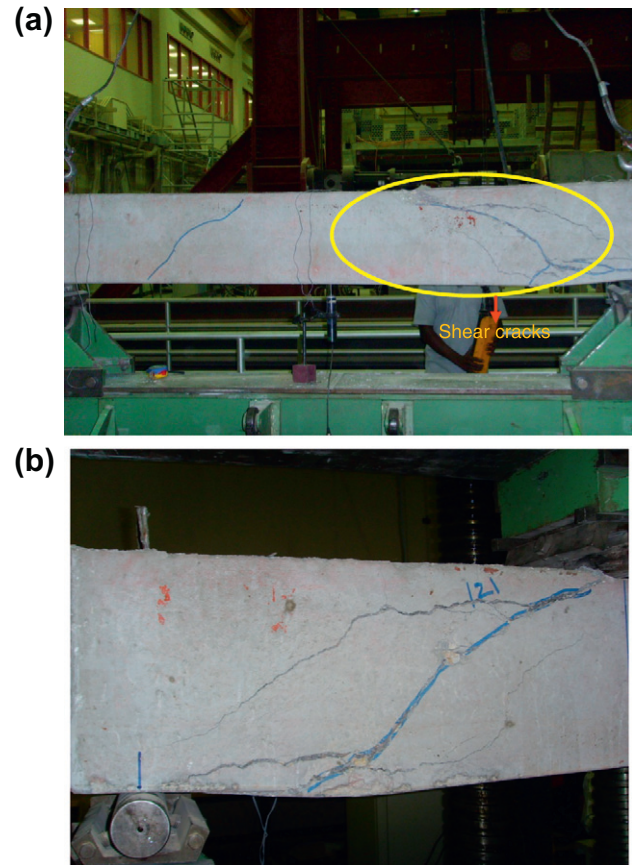


Fig. 8. Shear failure of the control beam specimen.

force is V_u and code-specified nominal shear capacity is V_n then the limit state function can be expressed as

$$g(\underline{x}) = V_n - V_u \quad (2)$$

From above equation it is obvious that brittle shear failure of RC beam will occur if V_n is equal to or less than V_u ; or $g(\underline{x})$ assumes a negative or zero value.

In the present study the nominal capacity of FRP upgraded shear-deficient beam was obtained by the equations proposed in ACI 440.2R-02 [18]. According to ACI 440.2R-02 [18] the nominal shear strength of an FRP-strengthened concrete member can be determined by adding the contribution of FRP reinforcement to the contributions from the reinforcing steel (stirrups, ties, or spirals) and the concrete as given below:

$$V_n = V_c + V_s + V_f \quad (3)$$

where V_c , V_s and V_f are the contribution of concrete, steel and FRP to shear strength. After substituting their expressions from Eqs. (A.2)–(A.4) (Appendix A), we have

$$V_n = \frac{\sqrt{f'_c}}{6} b_w d + \frac{A_v f_{ys} d}{S} + \frac{2n t_f w_f \epsilon_{fe} E_f (\sin \alpha + \cos \alpha) d_f}{s_f} \quad (4)$$

where b_w is the width of the beam; d the effective depth of beam section; A_v the area of steel stirrups; S the spacing between the stirrups; f'_c the compressive strength of concrete; f_{ys} the yield strength of steel stirrups; A_f the cross sectional area of FRP strip/sheet; ϵ_{fe} the effective strain in FRP laminates; α the angle of FRP strips from horizontal; d_f the effective depth of FRP strip/sheet; s_f the spacing between the two FRP strips; n the number of FRP plies or layers; t_f the thickness of FRP strip/sheet; w_f the width of the strip; E_f the

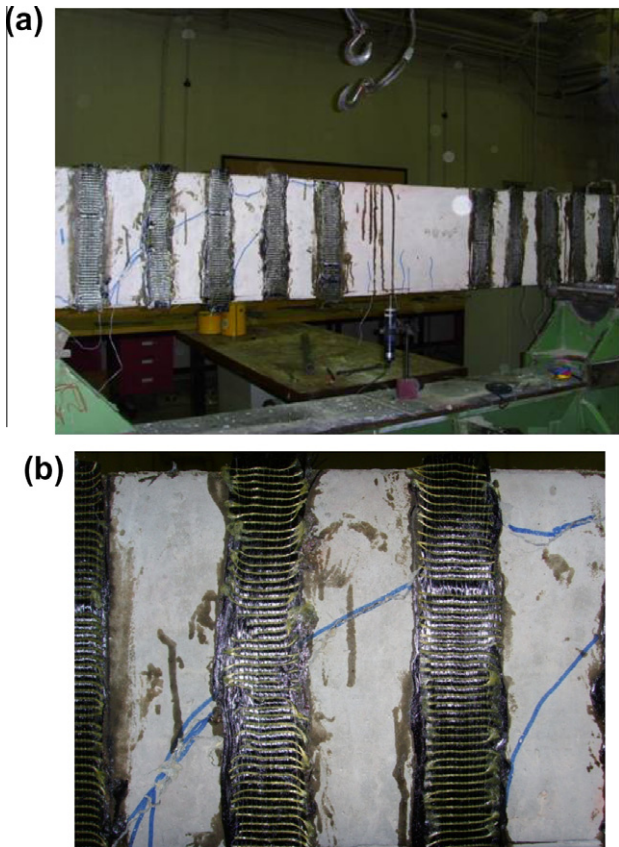


Fig. 9. Failure of the vertical-strip strengthened RC beam specimen.

FRP modulus of elasticity; and f_{fe} is the effective stress in FRP laminates.

The average effective strain in the FRP laminates (ϵ_{fe}) can be computed using the Eqs. (A.7)–(A.11) (Appendix A).

Having derived the limit state function the next step is the assessment of probability of failure (also called risk) and reliability (measured in terms of reliability index β) of the beams. For this purpose, Monte Carlo Simulation technique [19] has been employed. A brief description of this method is presented in the following section.

3.2. Monte Carlo simulation

Monte Carlo simulation consists of drawing samples of the basic random variables according to their probabilistic characteristics



Fig. 10. Failure of the inclined strip strengthened RC beam specimen.

and then feeding them into the limit state function. It is known that the failure occurs when $g(\underline{x}) < 0$; therefore an estimate of the probability of failure P_f can be found by

$$P_f = \frac{N_f}{N} \quad (5)$$

where N_f is the number of simulation cycles in which, $g(\underline{x}) < 0$, and N is the total number of simulation cycles. As N approaches infinity, the P_f approaches to the true probability of failure.

Having known the probability of failure, reliability index (β) can be determined using $\beta = -\Phi^{-1}(P_f)$, where P_f is the probability of failure and $\Phi^{-1}(\cdot)$ is the inverse of standard normal distribution function.

The accuracy of Eq. (5) can be evaluated in terms of its variance. For a small number of simulation cycles, the variance of P_f can be quite large. Consequently, it may require a large number of simulation cycles to achieve a specified accuracy. The variance of the estimated probability of failure can be computed by assuming each simulation cycle to constitute a Bernoulli trial. Therefore, the number of failures in N trials can be considered to follow a binomial distribution. Then the variance of the estimated probability of failure can be computed approximately as

$$\text{Var}(P_f) = \frac{(1 - P_f)P_f}{N} \quad (6)$$

It is recommended to measure the statistical accuracy of the estimated probability of failure by computing its coefficient of variation as:

$$\text{COV}(P_f) \cong \frac{\sqrt{\frac{(1 - P_f)P_f}{N}}}{P_f} \quad (7)$$

The smaller the coefficient of variation, the better is the accuracy of the estimated probability of failure. It is evident from Eqs. (6) and (7) that as N approaches infinity, $\text{Var}(P_f)$ and $\text{COV}(P_f)$ approaches zero. However, for all practical purposes, that number of simulation cycles for which $\text{COV}(P_f)$ approaches less than 5% may be considered as an appropriate number of simulation cycles [19].

The curves shown in Fig. 11 shows the variation of $\text{COV}(P_f)$ with the number of simulations for beam specimen strengthened using the inclined strips and subjected to the nominal service load as 60% of the tested beam capacity. This figure clearly illustrates that as the number of simulation cycles is increasing $\text{COV}(P_f)$ is decreasing. This convergence figure also suggests that, for the present problem, simulation numbers greater than 100,000 can yield a sufficiently accurate probability of failure. In the present study, therefore, 500,000 simulations were used to carry out the Monte Carlo Simulation for estimating the probabilities of failures.

In order to compare the probabilities of failure (P_f) and the reliability values (β), obtained for the shear mode of failure, probabilities of failure and reliability indices of the beams were also obtained against flexure mode of failure. In order to estimate P_f and β against flexure mode of failure, limit state function was defined as $g(\underline{x}) = M_n - M_u$. Here, M_n and M_u are the nominal moment capacity and the ultimate bending moment respectively.

3.3. Statistical data for reliability analysis

In order to carry out the reliability analysis of the beams, the variables which have substantial uncertainties have to be identified and their statistical characteristics including their meaningful probability distributions are required. The variables which are considered random along with their statistical properties and probability distributions are shown in Table 6. In this table, the bias factor represents the ratio of mean to the nominal value. When

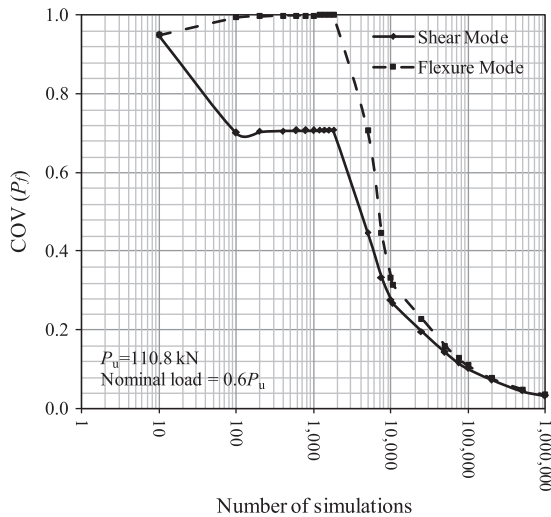


Fig. 11. Effect of simulation cycles on the convergence of P_f (P_u = average failure load).

bias factor is one, it indicates that the nominal value is same as the mean value. In general, for resistance related variables, bias factor is considered greater than one (i.e. in the design process, nominal value was taken less than the mean). Bias factor of less than 1.0 is generally assumed for load related variables.

To carry out the reliability analysis of RC beam specimens, a meaningful probability distribution for the expected extreme load is also necessary. In the present study randomness of the applied load was described using Extreme Type I distribution (Table 6). The coefficient of variation (COV) was considered to be equal to 25%. The probability distribution function (PDF) and the cumulative distribution function (CDF) for Extreme Type I distributed random variables are given by [19]:

$$\text{PDF} : f(x) = \alpha \exp\{-e^{-\alpha(x-u)}\} \exp\{-\alpha(x-u)\} \quad (8)$$

$$\text{CDF} : f(x) = \exp\{-e^{-\alpha(x-u)}\} \quad \text{for } -\infty \leq x \leq \infty \quad (9)$$

where u and α are distribution parameters. If the mean and standard deviation are known, values of the distribution parameters can be approximately estimated using [19]

$$\alpha \approx \frac{1.282}{\sigma_x} \quad (10)$$

$$u \approx \mu_x - 0.45\sigma_x \quad (11)$$

where μ_x and σ_x represent mean and standard deviation respectively. The references adopted for the selection of the COV and

the probability distributions of various random variables are shown in the last column of Table 6.

4. Discussion of results

Employing the data presented in Table 6 and using the Monte Carlo simulation technique, probability of failure and reliability indices of various beam specimens were obtained and shown in Table 7. In this table, the nominal applied load was varied as a fraction of ultimate load, obtained from the experiment, presented in the earlier section. The load was varied from $0.6P_u$ (approximately equal to service load) to P_u (equivalent to factored or ultimate load). The results clearly indicate that as the applied load is increasing probability of failure of the beam is also increasing. This is an expected trend.

Two last columns of Table 7 also list the values of the reliability indices (β) and the probabilities of failure (P_f) against the flexural mode of failure. A comparison of reliability index (β) values obtained by the reliability analysis of the beams against flexural and shear modes of failures indicate that for the control specimens the probabilities of failure are substantially higher in the shear mode of failure than the flexural mode. It is due to this reason the control beams were more likely to fail in the shear mode. This finding supports the failure mode obtained through the experiments, presented before. For beams, strengthened using vertical or inclined strips, although probabilities of failure are still higher for the shear mode of failure than the flexure mode of failure, but they are very close to each other. This also supports the experimentally observed failure mode and can be attributed to the fact that failure loads, shown in Tables 3 or 5, in the shear and the flexure modes are quite near to the each other.

The variations of reliability index with the applied load, ranging from working load to ultimate load are presented in Fig. 12. In these figures, a horizontal line is drawn corresponding to reliability index = 3.0. This index is designated as desired reliability index (β); since for the most structural components, a reliability index of 3.0 is a required reliability value [20–23]. These graphs illustrate that the control beams (Fig. 12) are deficient for all the applied load values as they are far below than the desired reliability index. Also, since there is a big gap between the reliability index values against the shear and the flexure modes of failures, the control beams are very well expected that they will fail in the shear mode. This observation supports the fact that the control specimens were failed in the shear without any indication of even impending flexural failure.

The beams strengthened using vertical or inclined strips are sufficiently reliable for applied nominal loads of 60 and 70 kN respectively. However, for loads higher than these values, beams are not reliable as desired. This figure also illustrates that for the applied loads, ranging from 50 kN to 120 kN, the beams strengthened with

Table 6
Random variables considered for the reliability analysis of the beam specimens.

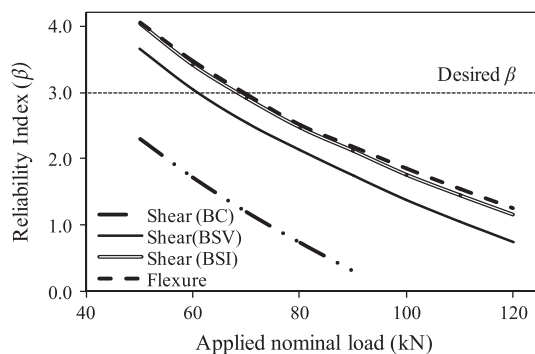
Random variable	Mean	Bias factor	COV	Distribution	Source (for COV and distribution)
Yield strength of longitudinal and transverse steel (f_y and f_{ys})	Nominal	1.10	0.125	Normal	[13]
Thickness of the CFRP strip (t_f)	1.0 mm	1.00	0.05	Lognormal	[14]
Depth to steel (d)	265 mm	1.00	0.03	Normal	[14]
Modulus of CFRP strips (E_f)	77 GPa	1.00	0.10	Lognormal	[14]
Inclination of CFRP strips	30°	1.00	0.05	Normal	Assumed
Spacing between CFRP strips (s_f)	150 mm	1.01	0.10	Normal	Assumed
Concrete strength (f'_c)	35 MPa	1.10	0.18	Normal	[14]
Beam width (b)	Nominal	1.00	0.03	Normal	[14]
CFRP strain at failure (ϵ_{fu})	1.1%	1.10	0.022	Weibull	[13]
Applied load	Variable	0.90	0.25	Extreme Type I	[14]

COV: coefficient of variation.

Table 7

Reliability indices and probabilities of failure of the beam specimens.

Beam specimen	Experimental failure load P_u (kN)	Applied nominal load (kN)	Against the shear mode of failure		Against the flexural mode of failure	
			β	P_f	β	P_f
BC	81.2	$0.6P_u$	2.38	8.74×10^{-3}	4.13	1.80×10^{-5}
		$0.7P_u$	1.90	2.89×10^{-2}	3.61	1.54×10^{-4}
		$0.8P_u$	1.46	7.22×10^{-2}	3.21	6.70×10^{-4}
		$0.9P_u$	1.06	1.45×10^{-1}	2.82	2.37×10^{-3}
		P_u	0.68	2.48×10^{-1}	2.47	6.71×10^{-3}
BSV	96.4	$0.6P_u$	3.54	2.00×10^{-4}	3.57	1.78×10^{-4}
		$0.7P_u$	3.04	1.20×10^{-3}	3.09	1.01×10^{-3}
		$0.8P_u$	2.60	4.70×10^{-3}	2.62	4.42×10^{-3}
		$0.9P_u$	2.23	1.30×10^{-2}	2.29	1.08×10^{-2}
		P_u	1.88	2.99×10^{-2}	1.96	2.53×10^{-2}
BSI	110.8	$0.6P_u$	3.09	9.98×10^{-4}	3.14	8.40×10^{-4}
		$0.7P_u$	2.57	5.06×10^{-3}	2.60	4.64×10^{-3}
		$0.8P_u$	2.16	1.53×10^{-2}	2.23	1.28×10^{-2}
		$0.9P_u$	1.77	3.80×10^{-2}	1.86	3.18×10^{-2}
		P_u	1.43	7.69×10^{-2}	1.52	6.41×10^{-2}

**Fig. 12.** Variation of the reliability index with the applied load.

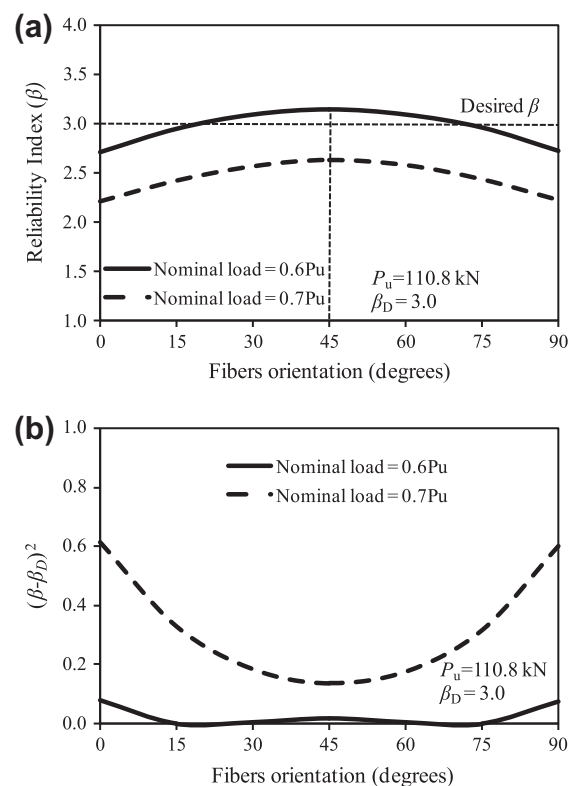
the inclined CFRP-strips are more reliable than the beams strengthened with the vertical strips. The reliability values of the beams strengthened with the inclined strips are very close to the reliability of the beams against flexure mode of failure. This can be attributed to the close values of failure loads in these two modes of failures as shown in Table 3.

5. Parametric study

In the following section three parametric studies (i) effect of fiber orientation; (ii) effect of strip-width and (iii) effect of strip-spacing on reliability index of shear strengthened RC beams have been carried out to arrive at the results of design interest. For the design purposes, the parameters should be selected in such a manner so that $(\beta - \beta_D)^2 \approx 0$. Here β and β_D are the actual and desired reliability index values. $(\beta - \beta_D)^2 \approx 0$ is an indication that the reliability of the beam is equal to the desired reliability value.

5.1. Effect of fiber orientation

Fig. 13 presents the variation of reliability index with fiber orientation of FRP strips. This figure clearly indicates that the beam has maximum reliability when CFRP fibers are oriented at 45°. This is due to the fact that the CFRP-strips contribute maximum to the shear strength when they are oriented at 45° (Eq. (4)). Fig. 13a illustrates that when the applied nominal load is 70% of the ultimate load, the specimen does not have the desired reliability at any value of the fiber orientation. However, when the applied load

**Fig. 13.** Variation of the reliability index with the fiber orientation.

is 60% of the ultimate load, the beam is sufficiently reliable for fiber orientation ranging from 30° to 60°. Therefore, in order to have the sufficient reliability for a shear-deficient beam subjected to approximately 60% of its ultimate capacity, CFRP strips should be attached to the beams at any angle from 30° to 60°. Fig. 13b also supports the same finding. That is, for fiber orientation of 30° to 60°, the shear deficient beams subjected to 60% of the nominal load gives the desired reliability. However, when the applied load is 70% of the ultimate load, the beam cannot achieve the desired safety just by attaching the CFRP strips at some angle. The desired reliability, in this case, can be achieved by altering the strip-width or strip-spacing or the both.

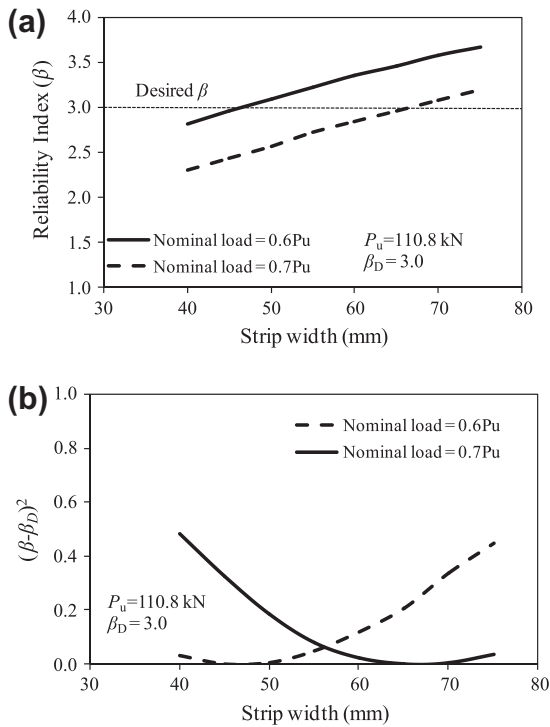


Fig. 14. Variation of the reliability index with the width of the CFRP-strips.

5.2. Effect of CFRP-strip-width

Fig. 14a shows the variation of reliability index with increase in the width of CFRP strips. It is very obvious that as the width of the strip increases the reliability increases almost linearly. This is due to the fact that the shear capacity of FRP-strengthened beam is

directly proportional to the strip width w_f (Eq. (4)). Fig. 14b shows the location where reliability of FRP-strengthened beam is equal to the desired reliability index ($=3$). When the applied nominal service load is 60% of the load carrying capacity of the strengthened beam, the required strip width is 50 mm. However, if the service load is 70% of the ultimate load, required width is about 70 mm.

5.3. Effect of CFRP-strip-spacing

Fig. 15a shows that as the spacing between the strips increases, reliability of the beam decreases almost linearly. This is due to the fact that as the spacing between the strips s_f increase, shear capacity decreases (Eq. (4)). Fig. 15b shows the spacing which is suitable for achieving the desired reliability index value of 3.0. If the applied service load is approximately 60% of the tested beam capacity, a spacing of 150 mm can give the desired reliability. However, if the applied load is 70% of the beam capacity, then the required spacing is 100 mm.

6. Conclusions

In the present study, a simple probabilistic procedure based on Monte Carlo Simulation technique was presented to study the reliability of shear-deficient control and the CFRP-strips strengthened RC beam specimens by varying the nominal applied load from $0.6P_u$ (approximately equal to service load) to P_u (equivalent to factored or ultimate load). The results clearly indicated that when the service load is 60% (or less) of the ultimate load, the CFRP-strips of width 50 mm, and center to center spacing of 150 mm can provide the desired reliability to the beam for any value of the fiber orientation ranging from 30° to 60° . However, when the service load is 70% (or more) of the ultimate load, it is difficult to achieve the desired reliability with the above configuration (width, spacing and orientation) of the CFRP-strips. The desired reliability, in this case, can be achieved by altering the strip-width or strip-spacing or the both.

The control beams are deficient for all the applied load values as their reliability index values are far below than the desired reliability index. Also, for these specimens there is a big gap between the reliability index values against the shear and the flexure modes of failures. This observation supports the fact that both the control specimens were failed in the shear mode without any indication of even impending flexural failure.

For beams, strengthened with vertical or inclined strips, although probabilities of failure are still higher for the shear mode of failure than the flexure mode of failure, but they are very close to each other. This again supports the experimentally observed failure mode.

The beams strengthened using vertical or inclined strips are sufficiently reliable for applied nominal loads of 60 and 70 kN respectively. However, for the loads higher than these values, beams are not reliable as desired. For the applied loads, ranging from 50 kN to 120 kN, the beams strengthened with the inclined CFRP-strips are more reliable than the beams strengthened with the vertical strips. The inclined CFRP-strips are thus much more effective in improving the reliability of shear-deficient beams than the vertical strips.

Acknowledgement

The work presented in this paper was funded by the Deanship of Scientific Research, Research Centre, College of Engineering, King Saud University, Riyadh, Saudi Arabia.

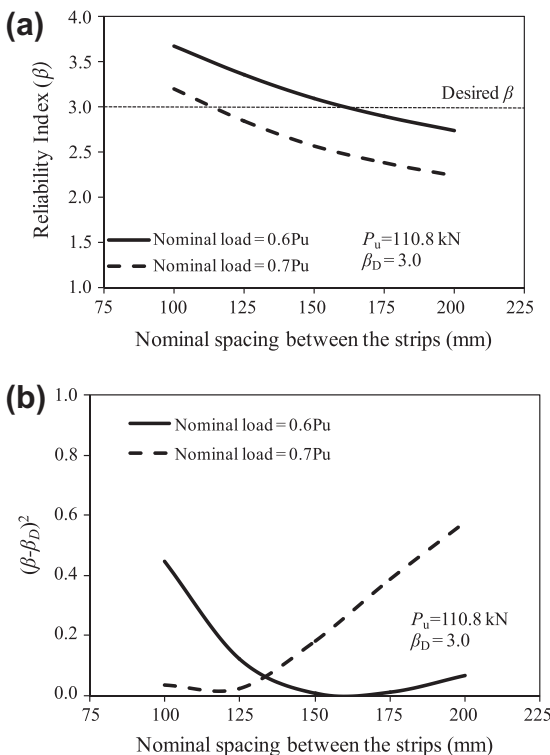


Fig. 15. Variation of the reliability index with the spacing between the CFRP-strips.

Appendix A. Shear strength of FRP strengthened beams

The nominal shear strength of an FRP-strengthened concrete member can be determined by adding the contribution of FRP reinforcement to the contributions from the reinforcing steel (stirrups, ties, or spirals) and the concrete as given below:

$$V_u = V_c + V_s + V_f \quad (A.1)$$

where V_c , V_s and V_f are the contribution of concrete, steel and FRP to shear strength. V_c and V_s can be computed by the following well known equations (ACI 318-2005)

$$V_c = \frac{\sqrt{f'_c}}{6} b_w d \quad (A.2)$$

$$V_s = \frac{A_v f_{ys} d}{S} \quad (A.3)$$

where b_w is the width of the beam; d the effective depth of beam section; A_v the area of steel stirrups; S the spacing between the stirrups; f'_c the compressive strength of concrete; and f_{ys} is the yield strength of steel stirrups. The contribution of FRP to shear strength can be estimated using the equation proposed by ACI 440.2R-02 (ACI 2002):

$$V_f = \frac{A_{fv} f_{fe} (\sin \alpha + \cos \alpha) d_f}{s_f} \quad (A.4)$$

$$\text{where } A_{fv} = 2nt_f w_f \quad (A.5)$$

$$\text{and } f_{fe} = \varepsilon_{fe} E_f \quad (A.6)$$

where A_{fv} is the cross sectional area of FRP strip/sheet; ε_{fe} the effective strain in FRP laminates; α the angle of FRP strips from horizontal; d_f the effective depth of FRP strip/sheet; s_f the spacing between the two FRP strips; n the number of FRP plies or layers; t_f the thickness of FRP strip/sheet; w_f the width of the strip; E_f the FRP modulus of elasticity; and f_{fe} is the effective stress in FRP laminates.

The effective strain in FRP laminates (f_{fe}) can be computed using the procedure proposed in ACI 440.2R-02 (ACI 2002). According to ACI 440.2R-02 (ACI 2002) procedure the effective strain, ε_{fe} in FRP is assumed to be smaller than the ultimate strain, ε_{fu} . This can be computed as

$$\varepsilon_{fe} = \begin{cases} 0.004 \leq 0.75 \varepsilon_{fu} & \text{for completely wrapped beams} \\ k_v \varepsilon_{fu} \leq 0.004 & \text{for two or three sides (e.g. U) bonded} \end{cases} \quad (A.7)$$

$$\text{where } k_v = \frac{k_1 k_2 L_e}{11900 \varepsilon_{fu}} \leq 0.75 \quad (A.8)$$

$$\text{Here, } L_e = \frac{23,300}{(nt_f E_f)^{0.58}} \quad (A.9)$$

$$k_1 = \left(\frac{f'_c}{27} \right)^{2/3} \quad (A.10)$$

$$k_2 = \begin{cases} \frac{d_f - L_e}{d_f} & \text{for U wraps} \\ \frac{d_f - 2L_e}{d_f} & \text{for two sides bonded} \end{cases} \quad (A.11)$$

where f'_c and E_f are in MPa.

References

- [1] Siddiqui NA. Experimental investigation of RC beams strengthened with externally bonded FRP composites. *Latin Am J Solids Struct (LAJSS)* 2009;6(4):343–62.
- [2] Alsayed SH, Almusallam TH, Al-Salloum YA, Siddiqui NA. Seismic rehabilitation of corner RC beam-column joints using CFRP composites. *J Compos Constr – ASCE* 2010;14(6):681–92.
- [3] Alsayed SH, Al-Salloum YA, Almusallam TH, Siddiqui NA. Seismic response of FRP-upgraded exterior RC beam-column joints. *J Compos Constr – ASCE* 2010;14(2):195–208.
- [4] Al-Salloum YA, Almusallam TH, Alsayed SH, Siddiqui NA. Seismic behavior of As-built, ACI-complying and CFRP-repaired exterior RC beam-column joints. *J Compos Constr – ASCE* 2011;15(4):522–34.
- [5] Al-Salloum YA, Siddiqui NA, Elsanadedy HM, Abadel AA, Aql MA. Textile-reinforced mortar (TRM) versus FRP as strengthening material of seismically deficient RC beam-column joints. *J Compos Constr – ASCE* 2011;15(6):920–33.
- [6] Triantafillou TC. Shear strengthening of reinforced concrete beams using epoxy-bonded FRP composites. *ACI Struct J* 1998;95(2):107–15.
- [7] American Concrete Institute (ACI). Guide for the design and construction of externally bonded FRP systems for strengthening concrete structures. ACI 440.2R-03, Farmington Hills, Michigan, USA; 2003.
- [8] Mofidi A, Chaallal O. Shear strengthening of RC beams with externally bonded FRP composites: effect of strip-width-to-strip-spacing ratio. *J Compos Constr – ASCE* 2011;15(5):732–42.
- [9] Razaqpur AG, Shedid M, Isgor B. Shear strength of fiber-reinforced polymer reinforced concrete beams subject to unsymmetric loading. *J Compos Constr – ASCE* 2011;15(4):500–12.
- [10] Bousselham A, Chaallal O. Maximum shear strength of RC beams retrofitted in shear with FRP composites. *J Compos Constr – ASCE* 2009;13(4):302–12.
- [11] Bousselham A, Chaallal O. Mechanisms of shear resistance of concrete beams strengthened in shear with externally bonded FRP. *J Compos Constr – ASCE* 2008;12(5):499–513.
- [12] Bae S, Murphy M, Mirmiran A, Belarbi A. Behavior of RC T-beams strengthened in shear with CFRP under cyclic loading. *J Bridge Eng – ASCE* 2013;18(2):99–109.
- [13] Okeil AM, El-Tawil S, Shahawy M. Flexural reliability of reinforced concrete bridge girders strengthened with carbon fiber-reinforced polymer laminates. *J Bridge Eng – ASCE* 2002;7(5):290–9.
- [14] Wiegand KT, Atadero RA. Effect of existing structure and FRP uncertainties on the reliability of FRP-based repair. *J Compos Constr – ASCE* 2011;15(4):635–43.
- [15] Monti G, Santini S. Reliability-based calibration of partial safety coefficients for fiber-reinforced plastic. *J Compos Constr – ASCE* 2002;6(3):162–7.
- [16] Plevris N, Triantafillou TC, Veneziano D. Reliability of RC members strengthened with CFRP laminates. *J Struct Eng – ASCE* 1995;121(7):1037–44.
- [17] American Concrete Institute (ACI). Building code requirements for structural concrete. ACI 318-05, Farmington Hills, Michigan, USA; 2005.
- [18] American Concrete Institute (ACI). Guide for the design and construction of externally bonded FRP systems for strengthening concrete structures. ACI 440.2R-02, Farmington Hills, Michigan, USA; 2002.
- [19] Nowak AS, Collins KR. Reliability of structures. 1st ed. Singapore: McGraw Hill; 2000.
- [20] Siddiqui NA, Iqbal MA, Abbas H, Paul DK. Reliability analysis of nuclear containment without metallic liners against jet aircraft crash. *Nucl Eng Des* 2003;224(1):11–21.
- [21] Choudhury M, Siddiqui NA, Abbas H. Reliability analysis of buried concrete target under missile impact. *Int J Impact Eng* 2002;27(8):791–806.
- [22] Siddiqui NA, Khan FH, Umar A. Reliability of underground concrete barriers against normal missile impact. *Comput Concr* 2009;6(1):79–93.
- [23] Khan RA, Siddiqui NA, Naqvi SQA, Ahmad S. Reliability analysis of TLP tethers under impulsive loading. *Reliab Eng Syst Saf* 2006;91(1):73–83.